

The origin of nematic order in FeSe

Andrey V. Chubukov¹, Rafael M. Fernandes¹, and Joerg Schmalian²

¹ *School of Physics and Astronomy, University of Minnesota, Minneapolis, MN 55455, USA*

² *Institute for Theory of Condensed Matter and Institute for Solid State Physics, Karlsruhe Institute of Technology, Karlsruhe, Germany 76131*

The origin of the 90 K nematic transition in the chalcogenide FeSe, which displays no magnetic order down to $T = 0$, remains a major puzzle for a unifying theory for the iron-based superconductors. We analyze this problem in light of recent experimental data which reveal very small Fermi pockets in this material. We show that the smallness of the Fermi energy leads to a near-degeneracy between magnetic fluctuations and fluctuations in the charge-current density-wave channel. While the two fluctuation modes cooperate to promote the same preemptive Ising-nematic order, they compete for primary order. We argue that this explains why in FeSe the nematic order emerges when the magnetic correlation length is smaller than in other Fe-based materials, and why no magnetism is observed. We discuss how pressure lifts this near-degeneracy, resulting in a non-monotonic dependence of the nematic transition with pressure, in agreement with experiments.

Nematic order in Fe-pnictides and Fe-chalcogenides develops at a temperature T_s that is larger than the magnetic transition (for reviews, see [1]). It spontaneously breaks the tetragonal C_4 lattice symmetry down to orthorhombic C_2 . The origin of this symmetry breaking is currently one of the most intensely debated issues of the Fe-based superconducting materials [2]. In the Fe-pnictides, nematic order occurs reasonably close to the instability towards stripe magnetic order at the Neel temperature T_N . Because the stripe order breaks Z_2 tetragonal symmetry ($C_4 \rightarrow C_2$) in addition to the $O(3)$ spin-rotational symmetry and because T_s and T_N show similar doping dependencies, it seems reasonable to associate the nematic order with magnetism [2]. Indeed, several groups have argued [3–12] that magnetic fluctuations split the mean-field stripe magnetic transition into two separate $O(3)$ and Z_2 transitions. The discrete Z_2 symmetry is broken first at $T_s > T_N$, resulting in an intermediate phase, dubbed Ising-nematic, where long-range magnetic order is absent but the C_4 lattice symmetry is broken down to C_2 . Such Z_2 order triggers orbital and structural order as all three break the same C_4 symmetry.

The magnetic scenario for nematicity in Fe-pnictides is supported by a variety of experimental observations, such as the doping dependencies of T_N and T_s [10], the scaling between the shear modulus and the spin-lattice relaxation rate [13], and the sign-change of the in-plane resistivity anisotropy between electron-doped and hole-doped Fe-pnictides [14]. This scenario, however, has been challenged for the Fe-chalcogenide FeSe. This material displays a nematic transition at $T_s \approx 90K$. The properties of the nematic phase in FeSe resemble those in Fe-pnictides: similar softening of the shear modulus [15], similar orthorhombic distortion and orbital order [16–18], and similar behavior of the resistivity anisotropy upon applied strain [19]. Furthermore, neutron scattering experiment shows that spin fluctuations are peaked at the same ordering vectors as in the Fe-pnictides [20, 21]. Yet, in distinction to Fe-pnictides, no magnetic order has thus far been observed in FeSe in the absence of external pres-

sure [22, 23]. Moreover, NMR measurements were interpreted as evidence that the magnetic correlation length ξ remains small at T_s [15, 24]. Although in the Ising-nematic scenario ξ *does not have to be large* at T_s , this seems to be the case for all Fe-pnictides.

Given these difficulties with the Ising-nematic scenario, spontaneous orbital order has been invoked to explain the nematic state in FeSe [15, 24]. However, at present, no microscopic theory exists where orbital order appears spontaneously instead of being induced by magnetism [25–29]. Alternative scenarios for magnetically-driven nematicity in FeSe have also been proposed, involving the formation of a quantum paramagnet [30], the onset of spin quadrupolar order [31], and strong frustration of the magnetic fluctuations [32]. Yet, the issue of why FeSe does not fit into a “universal” theory for the iron-based superconductors still persists.

In this communication, we present an extension of the spin-nematic scenario which explicitly builds on a unique property of the electronic structure of FeSe, namely, the fact that the Fermi energy E_F in this material is small – only a few meV, as seen by ARPES and dH-vA experiments [19, 33]. For a system with a small E_F , earlier renormalization-group (RG) calculations have shown that there are two density-wave channels whose fluctuations are strong at momenta $(0, \pi)/(\pi, 0)$: a spin density-wave (SDW) channel and a charge-current density-wave (CDW) channel (a CDW with imaginary order parameter, which we denote as iCDW [34]). The relative strength between the two depends on the sign of the inter-pocket exchange interaction (u_2 in our notations below). For repulsive u_2 , the coupling in the SDW channel is larger, while for attractive u_2 the coupling in the iCDW channel is larger. In both cases, however, the RG calculations show that the coupling in the subleading channel approaches the one in the leading channel at small energies. The RG process stops at E_F , implying that if E_F is larger than the highest instability temperature (T_s for FeSe) the subleading channel is not a strong competitor and for all practical purposes can be neglected. However,

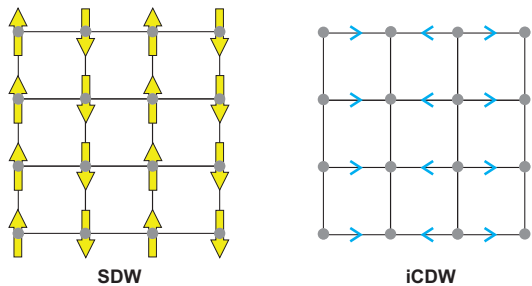


FIG. 1: Schematic representation of the SDW and iCDW ordered states with ordering vector $(\pi, 0)$. In the latter, the arrows represent charge currents along the bonds, while in the former, they represent spins on the sites. While fluctuations of both channels support nematicity, they compete for long-range magnetic and charge order.

if $E_F \sim T_s$, as in FeSe, the couplings in the two channels become degenerate within the RG. The degeneracy implies that the order parameter manifold increases from $O(3) \times Z_2$, for the three-component SDW, or from $Z_2 \times Z_2$, for the one-component iCDW, to a larger $O(4) \times Z_2$. In all cases, the Z_2 part of the manifold corresponds to selecting either $(0, \pi)$ or $(\pi, 0)$ for the density-wave ordering vector. While in both $O(3) \times Z_2$ and $O(4) \times Z_2$ models the Z_2 symmetry can be broken before the continuous one, in the latter this happens at a significantly smaller correlation length. As a result, at small E_F , the nematic order emerges while magnetic fluctuations are still weak. Furthermore, the SDW transition temperature T_N in the $O(4)$ model is additionally suppressed due to the competition with iCDW. We argue that these features explain the properties of the nematic state in FeSe, including non-monotonic pressure dependence of T_s [35, 36].

The model. We consider a quasi-2D itinerant band model with two hole pockets at the Γ point and two electron pockets at $(0, \pi)$ and $(\pi, 0)$ in the 1-Fe Brillouin zone [10, 37]. This model can be obtained from an underlying 5-orbital model with Hubbard and Hund interactions and hopping between the Fe $3d$ orbitals [38, 39].

The quadratic part of the Hamiltonian in the band basis describes the dispersion of the low-energy fermions, and the information about the orbital content along the Fermi pockets is passed onto inter-pocket and intra-pocket interactions, which are the Hubbard and Hund terms dressed by the matrix elements arising from the change from the orbital to the band basis [40]. The angular dependence of the matrix elements leads to angle-dependent interactions. The three interactions relevant for Ising-nematic order are the inter-pocket density-density interaction u_1 , the exchange interaction u_2 , and the pair-hopping interaction u_3 [41]. To simplify the analysis, we follow earlier works [10] and analyze the Ising-nematic order within an RG procedure that (i) approximates these three interactions as angle-independent and (ii) restricts the analysis to one hole pocket. The extension to two pockets and angle-dependent interactions makes the calculations more involved but does not

modify the RG equations in any substantial way and, moreover, leaves them intact if we treat the hole pockets as circular and neglect the d_{xy} orbital component on the electron pockets.

We label the fermions near the hole pocket as $c_{\mathbf{k}}$ and the fermions near the electron pockets as $f_{1,\mathbf{k}}$ and $f_{2,\mathbf{k}}$. The $O(3)$ magnetic order parameter is given by

$$\mathbf{M}_j = \frac{1}{N} \sum_{\mathbf{k}\alpha\beta} \left(c_{\mathbf{k},\alpha}^\dagger \boldsymbol{\sigma}_{\alpha\beta} f_{j,\mathbf{k}+\mathbf{Q}_j,\beta} + h.c. \right), \quad (1)$$

whereas the Z_2 iCDW order parameter is

$$\Phi_j = \frac{i}{N} \sum_{\mathbf{k}\alpha} \left(c_{\mathbf{k},\alpha}^\dagger f_{j,\mathbf{k}+\mathbf{Q}_j,\alpha} - h.c. \right), \quad (2)$$

with $j = 1, 2$ corresponding to the two possible ordering vectors $\mathbf{Q}_1 = (\pi, 0)$ and $\mathbf{Q}_2 = (0, \pi)$. We show these two ordered states in Fig. 1.

$O(4)$ Ising-nematic action. In the Ising-nematic scenario, the $C_4 \rightarrow C_2$ symmetry breaking implies the appearance of a composite order, quadratic in the density-wave order parameters \mathbf{M}_j and Φ_j . To analyze this scenario, we need to know the flow of the couplings that drive SDW order, $\Gamma_{\text{sdw}} = u_1 + u_3$, and iCDW order, $\Gamma_{\text{icdw}} = u_1 + u_3 - 2u_2$ (Ref. [41]). The bare coupling $\Gamma_{\text{sdw}} > \Gamma_{\text{icdw}}$ when $u_2 > 0$ and $\Gamma_{\text{icdw}} > \Gamma_{\text{sdw}}$ when $u_2 < 0$. As one integrates out the high-energy degrees of freedom via an RG procedure, the ratio $u_2/(u_1 + u_3)$ decreases as the system flows to lower energies (or temperatures) and approaches zero at the energy/temperature scale in which the system develops SDW/iCDW order. This holds, however, only if this scale is larger than E_F . If E_F is larger, the RG flow stops at E_F and the system develops an instability only in the channel with the largest bare coupling.

To illustrate our point, we plot in Fig. 2(a)-(b) the RG flow of Γ_{icdw} and Γ_{sdw} for a particular set of bare couplings $u_1(0) = u_2(0) = 10u_3(0)$, chosen deliberately to give a negative bare Γ_{icdw} . Under the RG flow, Γ_{icdw} becomes positive and approaches Γ_{sdw} at the scale where the couplings diverge and the system develops a density-wave order. The Fermi energy E_F sets the scale at which the RG flow stops. In case I (large E_F), the RG stops when Γ_{icdw} is still small. In case II (smaller E_F), the RG stop when Γ_{icdw} is comparable to Γ_{sdw} , and in case III (even smaller E_F), the RG flow reaches the $O(4)$ fixed point already at energies larger than E_F . We associate case I in Fig. 2 with Fe-pnictides, and cases II/III with FeSe based on the values of E_F obtained by ARPES and quantum oscillations [19, 33].

We next take the RG results as input and analyze the emergence of a nematic order which spontaneously breaks the symmetry between momenta \mathbf{Q}_1 and \mathbf{Q}_2 without breaking any other symmetry. The analysis follows the same steps as for pure SDW order [10]: we introduce \mathbf{M}_j and Φ_j ($j = 1, 2$) as Hubbard-Stratonovich fields which decouple the four-fermion interaction terms, integrate over the fermions, and obtain the effective action in terms of \mathbf{M}_j and Φ_j :

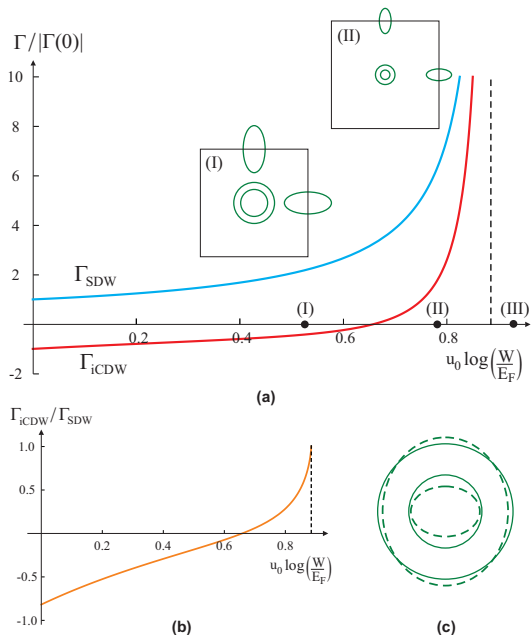


FIG. 2: (a) RG flow of the SDW and iCDW interactions Γ_{sdw} (red curve) and Γ_{icdw} (blue curve) as function of decreasing energy E . W is the bandwidth, $u_0 = u_1(0) = u_2(0) = 10u_3(0)$ is the bare interaction parameter, and the dashed line is the energy in which the two degenerate instabilities occur. The RG flow stops at the Fermi energy E_F : if E_F is large (case I, Fe-pnictides), only SDW fluctuations are relevant, whereas if E_F is small (cases II/III, FeSe), both SDW and iCDW fluctuations are important. The insets show schematically the Fermi pockets in each case. (b) Ratio $\Gamma_{\text{icdw}}/\Gamma_{\text{sdw}}$ along the RG flow. (c) Electronic manifestation of the Ising-nematic order on the hole pockets. There is a $\cos 2\theta$ distortion, with opposite signs for the two pockets, and an overall shift of the chemical potential.

$$S_{\text{eff}} = \int_{qj} (\chi_{s,q}^{-1} \mathbf{M}_j^2 + \chi_{c,q}^{-1} \Phi_j^2) + \frac{u}{2} \int_{xj} (\mathbf{M}_j^2 + \Phi_j^2)^2 - \frac{g}{2} \int_x [(\mathbf{M}_1^2 + \Phi_1^2) - (\mathbf{M}_2^2 + \Phi_2^2)]^2 \quad (3)$$

where $\chi_{s,q}^{-1} = \Gamma_{\text{sdw}}^{-1} - \Pi_q$ and $\chi_{c,q}^{-1} = \Gamma_{\text{icdw}}^{-1} - \Pi_q$ with $\Pi_q = \int_k G_{c,k+q} (G_{f_1,k} + G_{f_2,k})$. Note, the only asymmetry between the two order parameters is due to the interactions Γ_{sdw} and Γ_{icdw} , respectively. Near \mathbf{Q}_j , we can expand $\chi_{s(c),q}^{-1} \approx r_{0,s(c)} + \alpha(\mathbf{q} - \mathbf{Q}_j)^2$, where $r_{0,s(c)}$ measures the distance to the SDW (iCDW) mean-field instability and $\alpha \sim \mathcal{O}(1)$. The input from the RG analysis is that $r_{0,s}$ and $r_{0,c}$ are close to each other. The quartic coefficients are given by $(u, g) = \pm \frac{1}{2} \int_k G_{c,k}^2 (G_{f_1,k} \pm G_{f_2,k})^2$. At $\Gamma_{\text{sdw}} = \Gamma_{\text{icdw}}$, the action depends on \mathbf{M} and Φ only via the combination $\mathbf{M}^2 + \Phi^2$, and the order parameter manifold is $O(4) \times Z_2$. Evaluating the integrals at $E_F \sim T_s$, we find $u > 0$ and $g > 0$, what implies that long-range order selects either $j = 1$ or $j = 2$, but not both, i.e. it breaks both $O(4)$ and Z_2 symmetries.

Within a mean-field approximation, $O(4)$ and Z_2 are broken at the same temperature. Beyond mean-field, the Z_2 symmetry is broken first, and *both* \mathbf{M} and Φ contribute to it, even if $\Gamma_{\text{sdw}} \neq \Gamma_{\text{icdw}}$. To see this, we treat \mathbf{M} and Φ as fluctuating fields, introduce the composite fields $\psi = u(\mathbf{M}_x^2 + \Phi_x^2 + \mathbf{M}_y^2 + \Phi_y^2)$ and $\varphi = g(\mathbf{M}_x^2 + \Phi_x^2 - \mathbf{M}_y^2 - \Phi_y^2)$ to decouple the quartic terms, integrate over the primary fields \mathbf{M} and Φ and obtain the action in terms of ψ and φ :

$$S_{\text{eff}}[\varphi, \psi] = \frac{\varphi^2}{2g} - \frac{\psi^2}{2u} + \frac{3}{2} \int_q \ln [(\chi_s^{-1} + \psi)^2 - \varphi^2] + \frac{1}{2} \int_q \ln [(\chi_c^{-1} + \psi)^2 - \varphi^2] \quad (4)$$

The field ψ has a non-zero expectation value $\langle \psi \rangle \neq 0$ at any temperature as it does not break any symmetry, but only renormalizes the correlation lengths of the primary fields \mathbf{M} and Φ to $\xi_{s(c)}^{-2} = r_{0,s(c)} + \langle \psi \rangle$. A non-zero $\langle \varphi \rangle$, on the other hand, breaks the tetragonal C_4 symmetry. If this happens before the susceptibilities of the primary fields soften at \mathbf{Q}_j , then the Z_2 rotational symmetry breaks prior to other symmetry breakings. We emphasize that the nematic order parameter φ involves the combination $\mathbf{M}^2 + \Phi^2$, hence one cannot separate SDW induced and iCDW induced nematic order, even when χ_s and χ_c are not equivalent.

We solve the action in (4) within the saddle-point approximation, similarly to what was done in Refs.[10]. We find that at $\xi_s, \xi_c \approx \xi$, a non-zero nematic order parameter $\langle \varphi \rangle \neq 0$ emerges when the correlation length $\xi^2 = \pi/g$, or, to logarithmic accuracy in $g \ll 1$, at $T_s = 2\pi\rho_s/|\log g|$, where ρ_s is the stiffness of the $O(4)$ non-linear σ model associated with Eq. (3). It is instructive to compare this result with the case where only $O(3)$ SDW fluctuations are present. In that case, the nematic order emerges when $3\xi_{O(3)}^2 = 4\pi/g_{O(3)}$, and the transition temperature is $T_s = 2\pi\rho_s/|\log \sqrt{g_{O(3)}}|$, where $g_{O(3)}$ is the coupling in the SDW $O(3)$ model. As a result, to obtain the same T_s , one needs a much smaller coupling constant $g_{O(3)} \sim g_{O(4)}^2$. Consequently, at $T = T_s$, the correlation length $\xi_{O(4)}$ in the $O(4)$ case is proportional to $\xi_{O(4)} \sim \sqrt{\xi_{O(3)}}$, i.e. it is much smaller than it would be if nematicity was driven solely by SDW fluctuations. This is consistent with NMR [15, 24] and neutron scattering data [21] in the paramagnetic phase of FeSe, which point to the presence of SDW fluctuations, albeit weaker than in the Fe-pnictide compounds. The rapid increase of the correlation lengths below T_s , obeying $\xi_{s,c}^{-2} = \xi_{s,c}^{-2}(T_s) - \langle \varphi \rangle$, is also consistent with the increase of $1/T_1 T$ and the inelastic neutron signal [15, 21, 24].

The $O(4)$ Ising-nematic scenario also addresses why no magnetic order appears down to the lowest temperatures. The SDW and iCDW orders compete via the bi-quadratic term $(u - g) \mathbf{M}_j^2 \Phi_j^2$ in the low-energy action of Eq. (3). As a result, for $u_2 > 0$, fluctuations of the sub-leading iCDW channel suppress the transition temperature of the leading SDW channel. Such a suppression

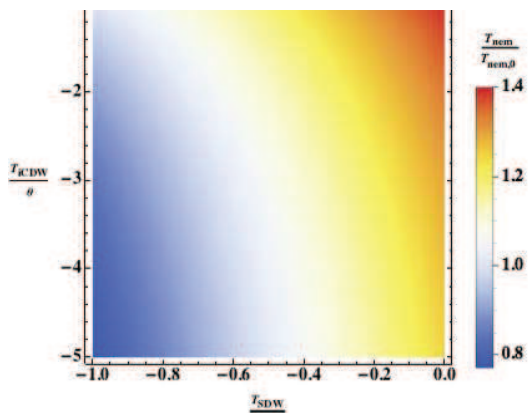


FIG. 3: Density plot of the nematic transition T_{nem} as function of the bare iCDW and SDW transitions T_{iCDW} and T_{SDW} . To mimic the effect of pressure, they start at the same negative value $-\theta$ at zero pressure, for which the nematic transition temperature is $T_{\text{nem},0}$, and then vary in opposite ways upon increasing pressure, $T_{\text{iCDW}} < -\theta$ and $T_{\text{SDW}} > -\theta$.

is the largest when the difference between the coupling constants $|\Gamma_{\text{sdw}} - \Gamma_{\text{icdw}}|$ is the smallest, which happens when the system flows towards $O(4)$ symmetry within RG, i.e. when E_F is small, such as in FeSe.

Experimental signatures. We now discuss the experimental consequences of the Ising-nematic order. The breaking of the Z_2 symmetry between the $j = 1$ and $j = 2$ components of the $O(4)$ field implies the breaking of C_4 lattice rotational symmetry down to C_2 . This instantaneously triggers structural order due to the coupling to lattice. To investigate how Z_2 order affects the electronic states, we return to the original four-pocket model (with fermions near the two hole pockets described by the operators $c_{1,\mathbf{k}}$ and $c_{2,\mathbf{k}}$) and include the explicit angle-dependence introduced by the matrix elements for the transformation between orbital and band basis. This transformation has the particularly simple form $c_{1,\mathbf{k}} = d_{xz} \cos \theta_{\mathbf{k}} - d_{yz} \sin \theta_{\mathbf{k}}$, $c_{2,\mathbf{k}} = d_{xz} \sin \theta_{\mathbf{k}} + d_{yz} \cos \theta_{\mathbf{k}}$ if one considers circular hole pockets and neglects the d_{xy} orbital component on the electron pockets [42]

The feedback effect of the Ising-nematic order on the fermions takes place via the self-energy corrections involving the unequal susceptibilities of the primary SDW and iCDW fields at momenta \mathbf{Q}_1 and \mathbf{Q}_2 . These corrections not only shift the chemical potentials of the f_1 and f_2 electron pockets in opposite directions $\langle f_{1,\mathbf{k}}^\dagger f_{1,\mathbf{k}} \rangle - \langle f_{2,\mathbf{k}}^\dagger f_{2,\mathbf{k}} \rangle \propto \langle \varphi \rangle$, but also give rise to a d -wave like distortion of the c_1 and c_2 hole pockets: $\langle c_{1,\mathbf{k}}^\dagger c_{1,\mathbf{k}} \rangle - \langle c_{2,\mathbf{k}}^\dagger c_{2,\mathbf{k}} \rangle \propto \langle \varphi \rangle \cos 2\theta_{\mathbf{k}}$ (see Fig.2b). In the orbital basis, the latter corresponds to ferro-orbital order $\langle d_{xz}^\dagger d_{xz} \rangle - \langle d_{yz}^\dagger d_{yz} \rangle \propto \langle \varphi \rangle$ [42]. Note that besides the changes in the dispersions proportional to $\langle \varphi \rangle$, there is an overall shift of the chemical potential, symmetric for the two electron and the two hole pockets.

The behavior of hole pockets in the Ising-nematic scenario is consistent with the existing ARPES data that show a d -wave type elongation of one of the hole pockets, whereas the other hole pocket sinks below the Fermi level [19]. The behavior of the electron pockets in the 2-Fe Brillouin zone is also consistent with the splitting of the chemical potentials of the f_1 and f_2 fermions.

We also investigate how pressure affects the nematic transition temperature T_s . Within our approach, T_s is defined by the condition $3\xi_s^2 + \xi_c^2 = 4\pi/g$. Upon pressure, the Fermi pockets become bigger, and the Fermi energy increases. As a result iCDW becomes less competitive and ξ_c decreases, while ξ_s increases. The combination of these two opposite tendencies in general gives rise to a non-monotonic behavior of T_s . This is illustrated in Fig. 3 using a simple modeling in which $\xi_j^{-2} \approx T - T_j$, with T_j denoting the bare transition temperatures for SDW and iCDW (see caption).

Note that in our analysis so far we considered $u_2(0) > 0$. If on the other hand this interaction is attractive, $u_2(0) < 0$, the iCDW phase is the leading instability, and the ground state manifold is $Z_2 \times Z_2$. In this case, the nematic and iCDW transitions are expected to be simultaneous [10]. Although at present no microscopic mechanism is known to give $u_2(0) < 0$ [34], this could be another possibility to explain the existence of nematic order without magnetic order in FeSe. Such an iCDW phase could be detected via its time-reversal symmetry breaking, which would be manifested in, e.g., μSR measurements. The phase diagram under pressure can be explained by assuming that under pressure u_2 would change sign and SDW would become the leading instability.

Summary In summary, we propose a natural extension of the Ising-nematic scenario to explain the puzzling nematic state observed in FeSe. Our scenario relies on the smallness of E_F and explains the onset of nematic order far from magnetism due to the near degeneracy between the SDW channel and an iCDW charge-current density wave channel. This near-degeneracy could result in the nucleation of local iCDW order in the presence of point-like impurities, which favor iCDW against SDW order [43]. While these fluctuations cooperate with magnetic ones to break the tetragonal symmetry, they compete for long-range order and reduce both T_N and the magnetic correlation length at the onset of nematic order. We argue that this Ising-nematic scenario can also explain the observed non-monotonic dependence of the nematic transition temperature T_s upon pressure.

We thank A. Boehmer, I. Fisher, P. Hirschfeld, U. Karahasanovic, J. Kang, S. Kivelson, I. Mazin, C. Meingast, R. Valenti, for useful discussions. This work was supported by the Office of Basic Energy Sciences U. S. Department of Energy under awards DE-FG02-ER46900 (AVC) and DE-SC0012336 (RMF) and the Deutsche Forschungsgemeinschaft through DFG-SPP 1458 *Hochtemperatursupraleitung in Eisenpniktiden* (JS).

-
- [1] D. C. Johnston, *Adv. Phys.*, **59**, 803 (2010); D.N. Basov and A.V. Chubukov, *Nature Physics* **7**, 241 (2011); J. Paglione and R. L. Greene, *Nature Phys.* **6**, 645 (2010); P. C. Canfield and S. L. Bud'ko, *Annu. Rev. Cond. Mat. Phys.* **1**, 27 (2010); H. H. Wen and S. Li, *Annu. Rev. Cond. Mat. Phys.* **2**, 121 (2011); P. Dai, J. Hu, and E. Dagotto, *Nature Phys.* **8**, 709 (2012).
- [2] R. M. Fernandes, A. V. Chubukov, and J. Schmalian, *Nature Phys.* **10**, 97 (2014).
- [3] C. Xu, M. Mueller, and S. Sachdev, *Phys. Rev. B* **78**, 020501(R) (2008).
- [4] C. Fang, H. Yao, W.-F. Tsai, J.P. Hu, and S. A. Kivelson, *Phys. Rev. B* **77** 224509 (2008).
- [5] E. Abrahams and Q. Si, *J. Phys.: Condens. Matter* **23**, 223201 (2011).
- [6] M. D. Johannes and I. I. Mazin, *Nature Phys.* **5**, 141 (2009).
- [7] Y. Kamiya, N. Kawashima, and C. D. Batista, *Phys. Rev. B* **84**, 214429 (2011).
- [8] M. Capati, M. Grilli, and J. Lorenzana, *Phys. Rev. B* **84**, 214520 (2011).
- [9] P. M. R. Brydon, J. Schmiedt, and C. Timm, *Phys. Rev. B* **84**, 214510 (2011).
- [10] R. M. Fernandes, A. V. Chubukov, J. Knolle, I. Eremin and J. Schmalian, *Phys. Rev. B* **85**, 024534 (2012).
- [11] S. Liang, A. Moreo, and E. Dagotto, *Phys. Rev. Lett.* **111**, 047004 (2013).
- [12] H. Yamase and R. Zeyher, arXiv:1503.07646.
- [13] R. M. Fernandes, A. E. Biçöçmer, C. Meingast, and J. Schmalian, *Phys. Rev. Lett.* **111**, 137001 (2013).
- [14] E. C. Blomberg, M. A. Tanatar, R. M. Fernandes, I. I. Mazin, B. Shen, H.-H. Wen, M. D. Johannes, J. Schmalian, and R. Prozorov, *Nature Comm.* **4**, 1914 (2013).
- [15] A. E. Biçöçmer, T. Arai, F. Hardy, T. Hattori, T. Iye, T. Wolf, H. v. Liçöçneysen, K. Ishida, and C. Meingast *Phys. Rev. Lett.* **114**, 027001 (2015).
- [16] K. Nakayama, Y. Miyata, G. N. Phan, T. Sato, Y. Tanabe, T. Urata, K. Tanigaki, and T. Takahashi *Phys. Rev. Lett.* **113**, 237001 (2014).
- [17] P. Zhang, T. Qian, P. Richard, X. P. Wang, H. Miao, B. Q. Lv, B. B. Fu, T. Wolf, C. Meingast, X. X. Wu, Z. Q. Wang, J. P. Hu, and H. Ding, arXiv:1503.01390.
- [18] Y. Zhang, M. Yi, Z.-K. Liu, W. Li, J. J. Lee, R. G. Moore, M. Hashimoto, N. Masamichi, H. Eisaki, S. -K. Mo, Z. Hussain, T. P. Devereaux, Z.-X. Shen, and D. H. Lu, arXiv:1503.01556.
- [19] M. D. Watson, T. K. Kim, A. A. Haghighirad, N. R. Davies, A. McCollam, A. Narayanan, S. F. Blake, Y. L. Chen, S. Ghannadzadeh, A. J. Schofield, M. Hoesch, C. Meingast, T. Wolf, and A. I. Coldea, arXiv:1502.02917.
- [20] M. C. Rahn, R. A. Ewings, S. J. Sedlmaier, S. J. Clarke, and A. T. Boothroyd, arXiv:1502.03838.
- [21] Q. Wang, Y. Shen, B. Pan, Y. Hao, M. Ma, F. Zhou, P. Steffens, K. Schmalzl, T. R. Forrest, M. Abdel-Hafiez, D. A. Chareev, A. N. Vasiliev, P. Bourges, Y. Sidis, H. Cao, and J. Zhao, arXiv:1502.07544.
- [22] T. M. McQueen *et al*, *Phys. Rev. Lett.* **103**, 057002 (2009).
- [23] T. Imai, K. Ahilan, F. L. Ning, T. M. McQueen, and R. J. Cava, *Phys. Rev. Lett.* **102**, 177005 (2009).
- [24] S.-H. Baek, D. V. Efremov, J. M. Ok, J. S. Kim, J. van den Brink, and B. Biçöçchner, *Nat. Mater.* **14**, 210 (2014).
- [25] C. C. Lee, W. G. Yin, and W. Ku, *Phys. Rev. Lett.* **103**, 267001 (2009)
- [26] C.-C. Chen, J. Maciejko, A. P. Sorini, B. Moritz, R. R. P. Singh, and T. P. Devereaux, *Phys. Rev. B* **82**, 100504 (2010)
- [27] W. Lv, F. Krüçeger, and P. Phillips, *Phys. Rev. B* **82**, 045125 (2010).
- [28] W.-C. Lee and P. W. Phillips, *Phys. Rev. B* **86**, 245113 (2012).
- [29] S. Onari H. and Kontani, *Phys. Rev. Lett.* **109**, 137001 (2012).
- [30] F. Wang, S. Kivelson, and D.-H. Lee, arXiv:1501.00844.
- [31] R. Yu and Q. Si, arXiv:1501.05926.
- [32] J. K. Glasbrenner, I. I. Mazin, H. O. Jeschke, P. J. Hirschfeld, and R. Valenti, arXiv:1501.04946.
- [33] T. Terashima *et al*, *Phys. Rev. B* **90**, 144517 (2014).
- [34] J. Kang and Z. Tesanovic, *Phys. Rev. B* **83**, 020505 (2011).
- [35] M. Bendele, A. Ichsanow, Y. Pashkevich, L. Keller, T. Strassle, A. Gusev, E. Pomjakushina, K. Conder, R. Khasanov, and H. Keller, *Phys. Rev. B* **85**, 064517 (2012).
- [36] T. Terashima, N. Kikugawa, S. Kasahara, T. Watashige, T. Shibauchi, Y. Matsuda, T. Wolf, A. E. Biçöçmer, F. Hardy, C. Meingast, H. v. Liçöçneysen, and S. Uji, arXiv:1502.03548.
- [37] I. Eremin and A. V. Chubukov, *Phys. Rev. B* **81**, 024511 (2010).
- [38] S. Graser, T. A. Maier, P. J. Hirschfeld, and D. J. Scalapino, *New J. Phys.* **11**, 025016 (2009).
- [39] The low-energy excitations in the band basis come from three orbitals – d_{xz} , d_{yz} , and d_{xy} . The two hole pockets are composed predominantly of d_{xz} and d_{yz} orbitals, and the two electron pockets of d_{xy} and d_{xz} orbitals ($(0, \pi)$ pocket) or d_{xy} and d_{yz} orbitals ($(\pi, 0)$ pocket).
- [40] L. Fanfarillo, A. Cortijo, and B. Valenzuela, arXiv:1410.8488.
- [41] A. V. Chubukov, D. Efremov, and I. Eremin, *Phys. Rev. B* **78**, 134512 (2008); A. V. Chubukov, *Physica C* **469**, 640 (2009); S. Maiti and A. V. Chubukov, *Phys. Rev. B* **82**, 214515 (2010).
- [42] R. M. Fernandes and O. Vafek, *Phys. Rev. B* **90**, 214514 (2014); V. Cvetkovic and O. Vafek, *Phys. Rev. B* **88**, 134510 (2013).
- [43] M. Hoyer, M. S. Scheurer, S. V. Syzranov, and J. Schmalian, *Phys. Rev. B* **91**, 054501 (2015).